SEISMIC BEHAVIOR OF A MULTISTORY AND MULTIBAY FRAME-INFILL SYSTEM

Ghassan Al-Chaar[1], Gregory E. Lamb[2], Daniel P. Abrams[3],

ABSTRACT

Even with recent advancements in the analysis of masonry-infilled frames, the seismic behavior of this complex structural system is not fully understood. Therefore, a three-story, three-bay R/C frame with URM infill model was subjected to a series of in-plane lateral forces to better understand its performance under seismic excitation.

The test specimen was a half-scale model designed from a building constructed in the 1950's. This building lacked the current seismic detailing typical of modern construction. A prescribed cyclic loading history placed displacement demands on the structure representative of those that are expected to occur during light, moderate, and strong earthquake motions. In this manner, knowledge of the behavior of this structural system under seismic loading was acquired.

Test results will be discussed in this paper with respect to measurements of strength, stiffness and deformation capacity as well as observed damage patterns and apparent performance limit states. Propagation of cracks in the concrete frame and masonry infill during the loading will be illustrated and discussed with respect to measured histories of force and deflection. Measured shear strains in each of the nine infill panels will also be correlated with the progression of damage to infer the distribution of lateral force to each infill panel.

Key words: Cyclic Loading, Multibay, Multistory, Reinforced Concrete, Seismic, Stiffness, Strength, Unreinforced Masonry.

[1] Research Structural Engineer, USAERDC, P.O. Box 9005, Champaign, Illinois 61826-9005
g-al-chaar@cecer.army.mil
[2] Graduate Research Assistant, University of Illinois at Urbana-Champaign
1203 Clifford Dr., Apt. 5, Urbana, Illinois 61802
glamb@uiuc.edu
[3] Hanson Engineers Professor of Civil Engineering,
University of Illinois at Urbana-champaign
1245 Newmark Civil Engineering Laboratory, 205 North Mathews Avenue
Urbana, Illinois 61801
d-abrams@uiuc.edu

were placed on each floor of the half-scale specimen. Approximately 4.38 N/mm of additional vertical load per floor was applied in this method. Once the lead ingots were in place, a cyclic loading protocol for the third floor was chosen. Several methods were considered, but the CUREe method (Krawinkler 2000) seemed best suited for the testing of the half-scale model. This method incorporated trailing cycles which stabilize the force-displacement relationship before reaching the next primary cycle.

After choosing the CUREe loading history, a few modifications to the method needed to be implemented. Adjustments allowing for a test duration of three hours, a maximum third floor displacement of three inches, and 40 complete cycles were employed. Selecting a maximum third floor displacement of three inches along with 40 complete cycles was incorporated to ensure that sufficient degradation of strength had occurred by the completion of the test. The test length of approximately three hours was chosen in order to allow for adequate time to monitor test data and specimen performance during the test. The resulting cyclic loading history is presented in Figure 2. The drift ratio, as used in Figure 2, refers to the third floor displacement over the entire height of the half-scale model.

After choosing a displacement history for the third floor, a method of force-controlled loading was established for the first and second floors. As the third floor was displaced according to the Modified CUREe loading history, the ratio of load placed on the first and second floors relative to the third floor was kept constant. This ratio was based on the vertical distribution of mass contributing to seismic forces and was calculated according to the International Building Code 2000. The load ratios gave an approximate inverse triangular vertical distribution of lateral seismic force.

EXPERIMENTAL RESULTS

Material Properties

Comprehensive material testing was conducted in order to find the engineering properties of the construction materials used for the experimental model. The most important of these values are given in Table 1.

Table 1. Material Properties.

Floor	Concrete Compressive Strength (kPa)	Masonry Prism Strength (kPa)	Steel Reinforcing Bars	Nominal Area (mm^2)	Yield Strength (MPa)
1	33410	5426	D2	13	324
2	30100	6743	#3	71	427
3	18060	6019	6 gage	18	400

Load-Deflection Behavior

Applying the proposed loading histories on the test specimen resulted in the force-deflection relations shown in Figure 3. The load plotted on the ordinate is the accumulated story shear for each floor level. The drift ratio, plotted on the abscissa, is defined as the interstory displacement divided by the story height given as a percent. The hysteresis for each floor will be discussed in order to explain the behavior of the test specimen.

The peak load for the experimental model occurred during the 21st cycle at a corresponding first floor story shear of 143.28 kN. The second and third floors had story shears of 110.76 and 63.03 kN, respectively, during the positive stroke of this cycle. During the negative stroke, the story shear for the first, second, and third floors were 129.08, 102.66, and 61.83 kN, correspondingly. The associated drift ratios at peak load in the positive stroke direction were 0.115%, 0.207%, and 0.069% for the respective floors. For the negative stroke direction, values of 0.088%, 0.354%, and 0.054% occurred for the drift ratio in the first, second, and third floors, accordingly. These values, along with the applied peak load for each floor, are summarized in Table 2.

Table 2. Peak Load and corresponding Story Shear and Drift Ratio for each floor.

	Peak Load (kN)		Story Shear (kN)		Drift Ratio (%)	
Floor	+	-	+	-	+	-
3	63.03	61.83	63.03	61.83	0.069	0.054
2	47.73	40.83	110.76	102.66	0.207	0.354
1	32.52	26.42	143.28	129.08	0.115	0.088

Note: + and - refer to the direction towards and away from the reaction structure, respectively.

The remaining 19 cycles, up to an absolute third floor displacement of three inches, were sufficient in reaching the residual strength of the test specimen. The drift ratios and associated lateral loads during the last primary cycle (cycle 38) are summarized in Table 3.

Table 3. Maximum Drift Ratio and corresponding Load for each floor.

	Lateral Load (kN)		Max. Drift Ratio (%)	
Floor	+	-	+	-
3	48.44	46.75	0.488	0.186
2	35.99	30.25	2.083	2.667
1	25.58	18.64	2.088	1.979

From Figure 3, the drift ratio of the third floor after the peak load was much less than the values observed in the first or second floors. The main cause of this behavior was due to

the prescribed inverse triangular distribution of lateral forces specified in IBC 2000 and the resulting story shear distribution shown in Table 4. The story shear on the first and second floors was roughly double the value applied to the third floor. This story shear distribution caused the drift ratios for the first and second floors to be much greater than the third floor. The relatively high values of drift ratio in the lower levels caused these panels to crack first. Once cracked, the difference in drift ratio between the third floor and the lower levels was amplified.

The prescribed distribution of story shear was also one of the causes of the first masonry cracks developing on the second floor rather than the first floor at the peak load. During the peak load, cracks emerged in every masonry panel on the second floor, while only one crack appeared in the masonry on the first floor. In addition to the vertical distribution of story shear, the possibly more important factor that caused this behavior was the distribution of vertical load from the dead weight of the test specimen and the lead ingots. Each floor was loaded similarly, leading to the accumulated vertical load distribution given in Table 4.

The total vertical load on the first floor was 1.5 times the value of the second floor. However, the story shear in the first floor was only 1.27 times the value of the second. The large increase in accumulated vertical load relative to story shear from the second to the first floor was one explanation for only one crack appearing in the first floor during the peak load. Conversely, the second floor, with one-third less total vertical load, still experienced a relatively large story shear of approximately 79% of the first floor value. This large story shear coupled with a smaller vertical load decreased the lateral load capacity of the second floor. Therefore, significant cracking occurred on this level during the peak load.

Table 4. Lateral Load, Story Shear, and Vertical Load Distribution for each floor.

Floor	Lateral Load Distribution (% of V)	Story Shear Distribution (% of V)	Accum. Vertical Load Distribution (% of P)
3	46%	46%	33%
2	33%	79%	67%
1	21%	100%	100%

Note: V represents the Base Shear, and P symbolizes the Total Applied Vertical Load.

After cracking occurred in floors one and two, the imposed displacement on the third level from the Modified CUREe load protocol was mostly taken from these lower levels. The cracking of the masonry panels in the lower levels caused a significant loss in stiffness for floors one and two. This caused the majority of the displacement required of the third floor to be captured by the first and second floors. Therefore, the large increase in drift ratio for the first and second floors after peak load and the relatively small increases in drift ratio for the third floor during this time, as shown in Figure 3, can be explicated by this phenomenon. In addition, the observation of relatively few cracks in the third floor during testing was consistent with the small values of drift ratio achieved on this floor. Furthermore, the distribution of displacements, as a percentage of the third floor displacement, before and after cracking is shown in Table 5. After cracking, the

displacement distribution increased by 71% and 21% in the first and second floors, respectively. This illustrates that the accumulation of displacements in the first and second floors after cracking caused the minimal additional accrual of drift ratio in the third floor after the peak load.

Table 5. Displacement Distribution (% of 3rd Floor) before and after Cracking.

Floor	Before Cracking	After Cracking	Percent Increase
3	100 %	100 %	0
2	80 %	97 %	21 %
1	23 %	40 %	71 %

The significant cracking in floors one and two also caused the hysteresis of floor three to become asymmetric as shown in Figure 3. The negative drift ratio of the third floor hysteresis was much less than the drift ratio in the positive direction. The main cause of this asymmetry stemmed from the considerable cracking in the lower-left quadrant of the second floor masonry panels observed during testing and illustrated in Figure 4. These cracks near the toe of the masonry panels caused a considerable decrease in stiffness of the second floor in the negative stroke direction, i.e. in the direction away from the reaction structure. In effect, the second floor attracted the most interstory displacement in the negative stroke direction after cracking. This phenomenon left the third floor with little needed additional drift in order to comply with the specified displacement from the loading protocol.

Besides examining the hysteresis curves, another method for investigating stiffness degradation was utilized in this experiment. Stiffness for each primary cycle, starting with cycle 14, was calculated by measuring the slope of a straight line connecting the peak load during that cycle to the origin of a story shear versus interstory displacement graph. Using this method, values of "stiffness" for each primary cycle for both stroke directions were computed and summarized in Table 6. The average stiffness is computed as the average of the stiffness in the positive and negative stroke directions.

Table 6. Stiffness (kN/mm) of each floor during Primary Cycles.

Cycle	First Floor			Second Floor			Third Floor		
No.	+	-	Average	+	-	Average	+	-	Average
14	237	175	206	67	54	61	121	102	112
21	85	95	90	37	19	28	60	74	67
25	38	44	41	20	12	16	33	61	47
29	26	29	27	12	8	10	28	48	38
32	12	18	15	7	4	6	16	31	23
35	7	7	7	4	3	4	9	20	14
38	4	3	3	3	2	2	6	16	11

This table illustrates the stiffness degradation which occurred throughout the extent of the test. All floors showed significant loss of stiffness by the completion of the test. The percent of initial stiffness remaining by cycle 38 for floors one, two, and three were 1%, 3%, and 10%, respectively. This exemplifies the concentration of damage to the first and second floors, while the third floor remained mostly intact. One interesting note, the initial stiffness (cycle 14) of the second floor was considerably less than that of floors one and three. No reasonable explanation can be given in view of the fact that the material tests performed for the second floor showed no signs of weak materials.

Diagonal Masonry Panel Strain Distribution

The diagonal strain distribution in the masonry panels will be discussed in order to infer the distribution of lateral force. Location of panels with large diagonal deformations will be found from the data. Strain distributions at peak load and cycle 29 will be discussed. Cycle 29 imposed panel displacements of 5 mm, which was the maximum range of the LVDTs. Therefore, readings after this cycle were inconclusive. Since only one LVDT was used for each panel, compressive displacements were obtained only in the positive stroke direction. Therefore, only masonry panel strain distributions in this direction will be discussed. The values of panel strain were normalized to the panel which had the largest displacement during that cycle. Therefore, a value of 100% represents the panel which had the largest displacement, and a value of 50% signifies a diagonal panel displacement of half of the maximum during that cycle. The masonry panel identification scheme used in this section is shown in Figure 5.

From Figure 6, the panel strain distribution at peak load during the positive stroke cycle is shown normalized to panel 2A. The observation of the first cracks occurring in the second floor during this cycle, especially the center panel, was consistent with the large strains on this level. Another observation is the strain in Bay A was larger in magnitude than the strain in Bay C for the first and second floors. This difference in strain can be attributed to the overturning moment from the application of the loading history. The combination of vertical load, lateral force, and overturning moment caused strains in the lower levels of Bay A to be appreciably larger than the corresponding strains in Bay C. The strain in Panel 2A was approximately 38% larger than the value for Panel 2C. On the first floor, where the overturning moment was at a maximum, the strain in Panel 1A was roughly 170% larger than the value in Panel 1C. Conversely, in the third story, where the vertical and lateral load was at a minimum, the overturning moment was negligible and resulted in relatively small strains in Panels 3A and 3C.

In Figure 7, the panel strain distribution for cycle 29 is given. Diagonal panel displacements of 5 mm, the maximum range of the LVDTs, were achieved during this cycle. The strain in each panel was normalized to panel 2A, which once again had the highest recorded value of displacement.

The strain distribution during cycle 29 mimicked the behavior seen during the peak load. The largest deformations once again occurred on the second floor. Furthermore, the lopsided distribution of panel strain due to overturning moment effects was also still present. However, this effect was only appreciable in the first story during this cycle where Panel 1A had almost 3 times the deformation as Panel 1C. The third floor masonry panels remained generally unaffected by the loading history with relatively small strains and no perceivable overturning moment effects.

CONCLUSIONS

This paper presented the results from the cyclic loading of a three-story, three-bay R/C frame with URM infill half-scale model. Discussion was provided to assist in understanding the behavior of this complex structural system. The successful completion of this test provided the following conclusions.

1. Behavior was dominated by the R/C frame, with cracking of the unreinforced concrete masonry infills following distortions of the frame. Thus, undesirable forces were not perceivably delivered to the frames from the infills, which could be the case with stronger and stiffer panels.
2. Damage to the R/C frame consisted of flexural and shear cracking of the concrete, and yield of reinforcement in the beams and columns. A follow-up investigation is examining the effectiveness of repair measures for these members.
3. Despite the non-ductile detailing of frame reinforcement, the shape of the overall force-deflection relations were similar to those for frames with more modern detailing, though strength and stiffness deterioration was more pronounced with the 1950-vintage construction.

REFERENCES

ACI Committee 318, "Building Code Requirements for Reinforced Concrete (ACI 318-51)" American Concrete Institute, Detroit, Mich., 1951.

International Code Council (2000), *International Building Code 2000*, Virginia.

Krawinkler, H., Parisi, F., Ibarra, L., Ayoub, A., Ricardo, M. "Development of a Testing Protocol for Wood Frame Structures," Stanford University, April 2000 draft.

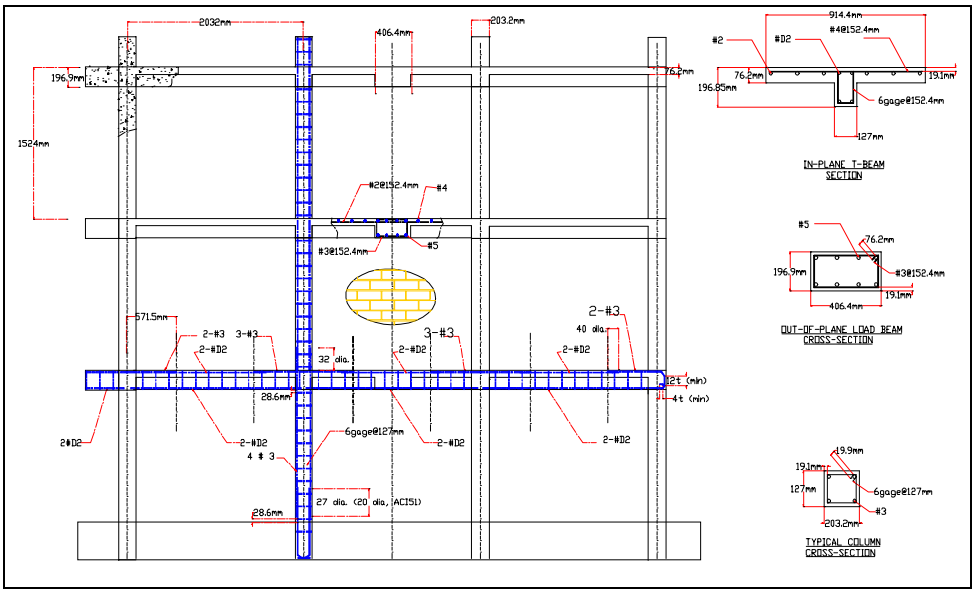

Figure 1. Half-Scale Experimental Model.

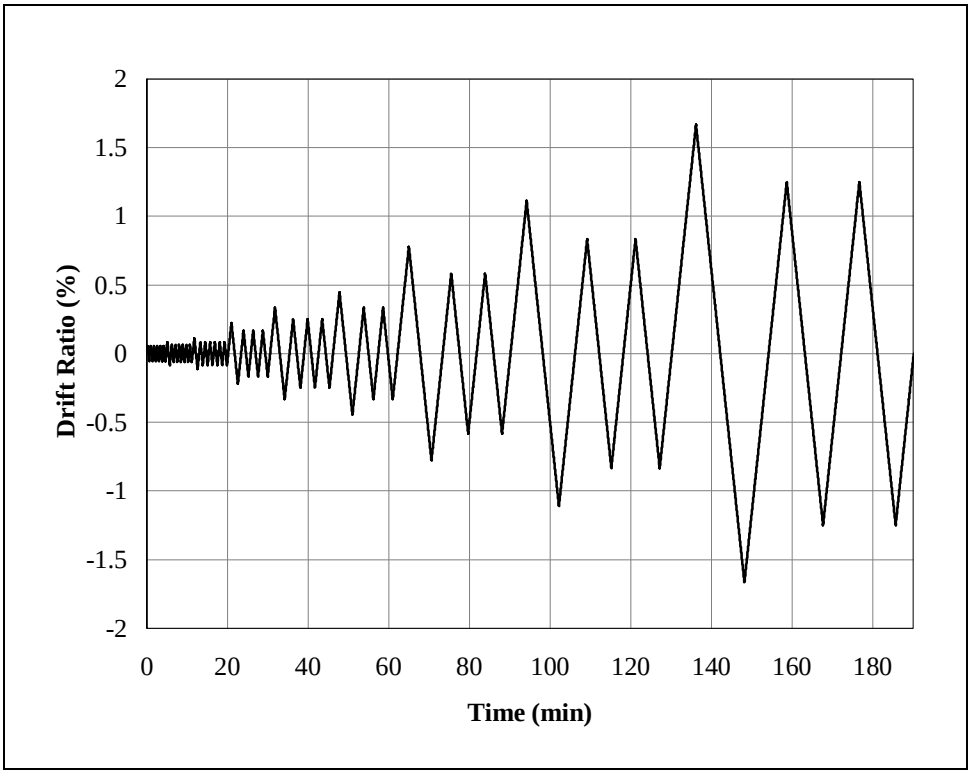

Figure 2. Modified CUREe Loading History.

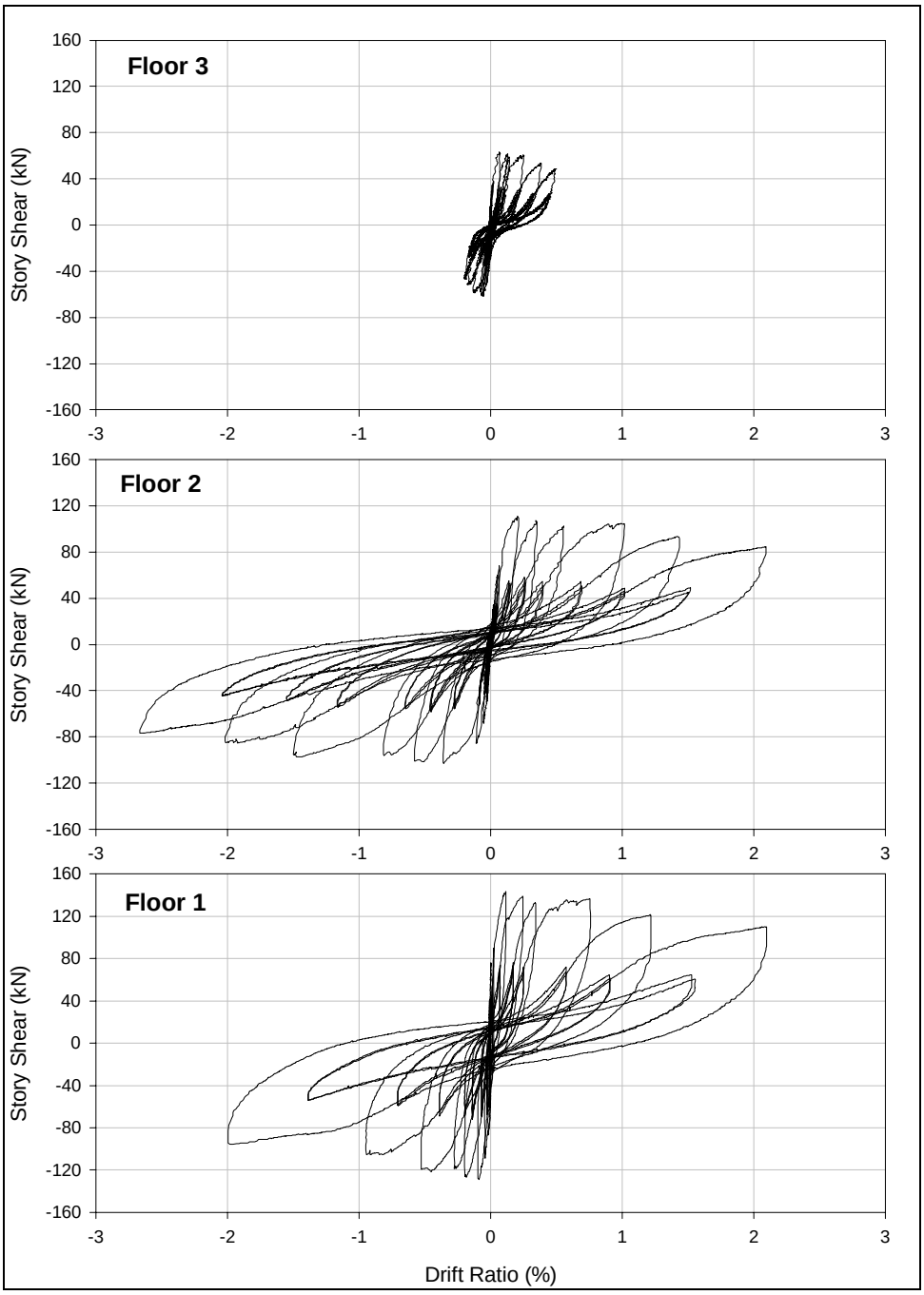

Figure 3. Story Shear versus Drift Ratio for Floors 1 through 3.

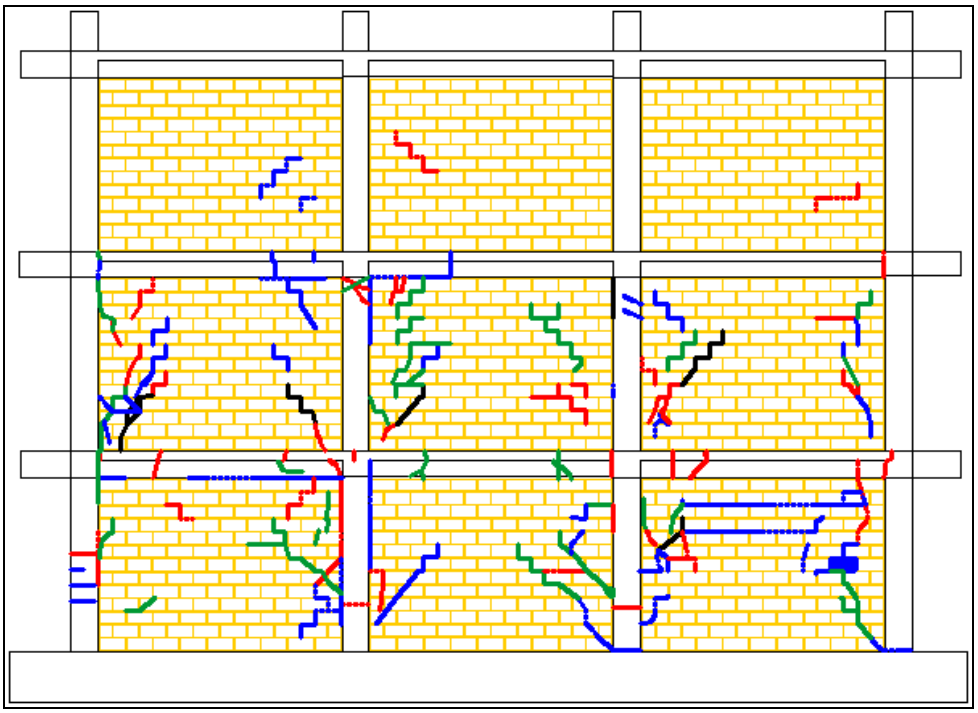

Figure 4. Cracking in Experimental Model during Testing.

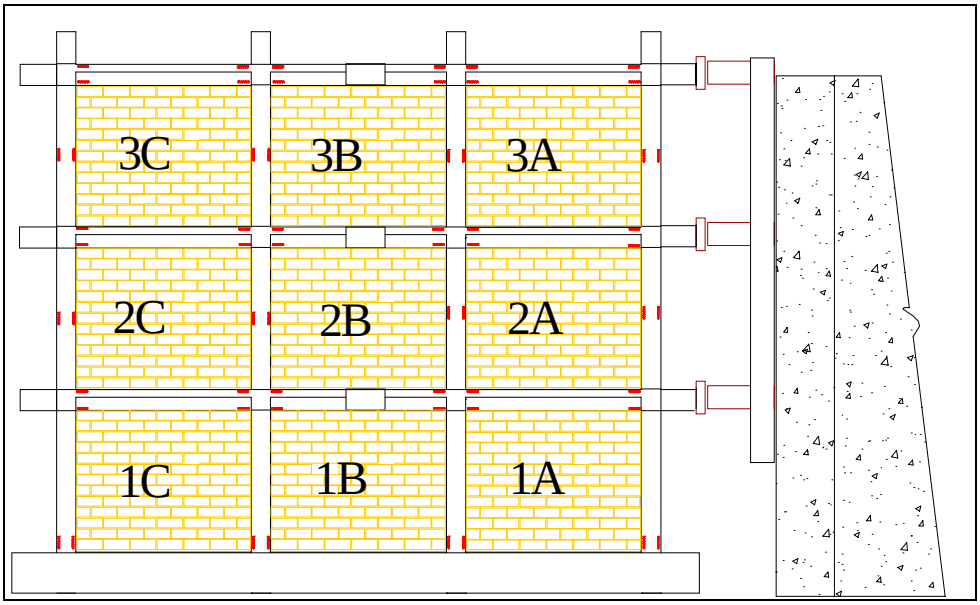

Figure 5. Identification Scheme used for the masonry panels.

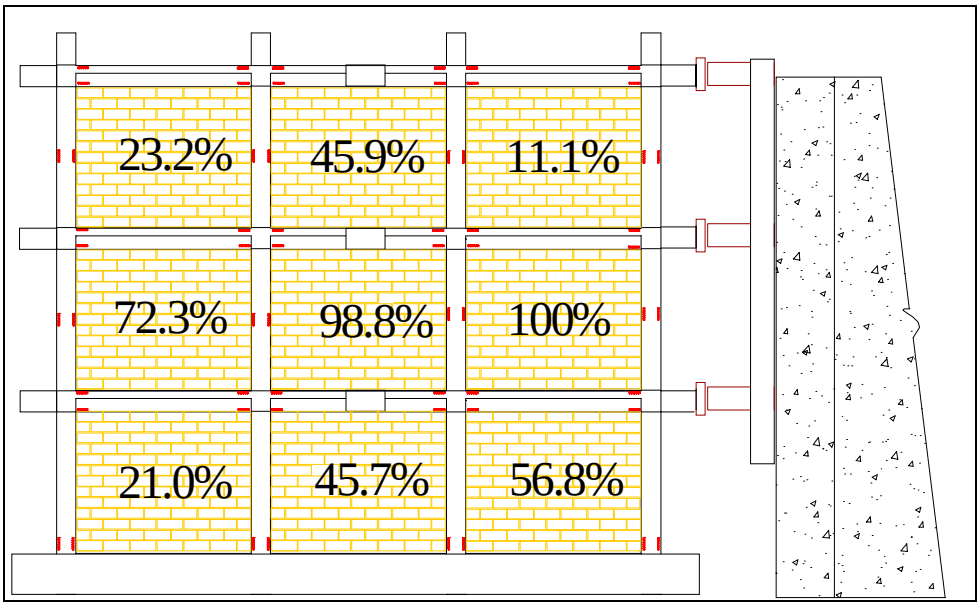

Figure 6. Panel Strain Distribution at Peak Load (Cycle 21).

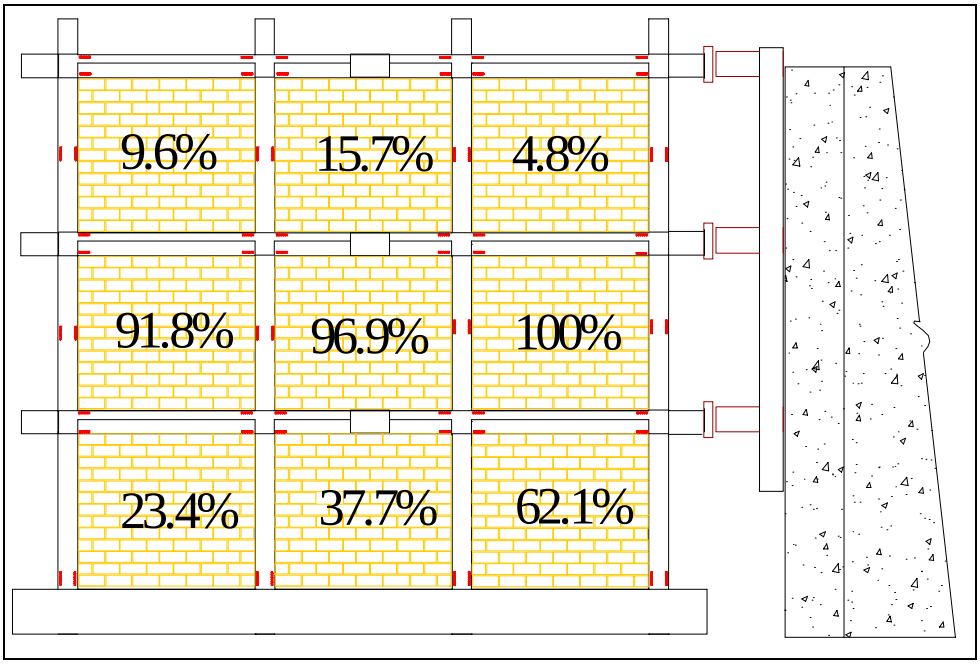

Figure 7. Panel Strain Distribution during Cycle 29.